



Methodology for electromagnetic analysis using the finite element method for fusion reactor components

A. Fernández^{a,c,*}, J. Martínez-Fernández^a, M. Medrano^a, S. Cabrera^a, P. Testoni^b, E. Rodríguez^c

^a Laboratorio Nacional de Fusión, CIEMAT, 28040 Madrid, Spain

^b F4E, Josep Pla 2, Torres Diagonal Litoral B3, 08019 Barcelona, Spain

^c Department of Construction and Manufacturing Engineering, University of Oviedo, Campus de Gijón, 33203 Gijón, Spain

ARTICLE INFO

Keywords:

Electromagnetic analysis
FEM
Fusion reactor components
ITER diagnostic
WAVS

ABSTRACT

Electromagnetic (EM) analyses are carried out when designing fusion reactor components to verify that they withstand the EM loads developed during transient plasma events, thus ensuring their proper functioning.

A complete methodology has been developed to conduct EM analyses by creating algorithms to guide the analyst during the decisions and actions to be taken, from the selection of the case events and the calculation method to the validation of the final results. This methodology has been applied to the EM analyses of the ex-vessel components of the ITER diagnostic Wide-Angle Viewing System (WAVS) in its final design stage. The calculation method selected is the Spheres-Worst instant method, implemented with a 3D finite element model. The paper includes a verification analysis of the simplifications made and a method to optimize the resources needed for the EM analysis.

1. Introduction

Magnetic confinement fusion reactors, like the one of the ITER project, are exposed to intense magnetic fields generated by powerful superconducting magnets. Certain transient plasma events, like Vertical Displacement Events (VDE) or Major Disruptions (MD), cause a sudden magnetic field variation, inducing eddy currents in the electrically conductive components [1]. Volumetric forces arise in these components from the interaction of the eddy currents with the surrounding magnetic field.

Electromagnetic (EM) analyses are carried out when designing reactor components to verify that they withstand the EM loads developed during the stated events, thus ensuring their proper functioning.

There are many ways to perform an EM analysis. The selection of the case events to simulate, the calculation method, the components to be modelled and the procedure followed during the analysis are usually defined ad hoc for each project and depend on the study goals, on the required accuracy of results and on the available resources. When it comes to the calculation method, if considering the contributions from global sources is required, the model of complete tokamak sectors is frequently included. For example, in [2], a complete 40° ITER sector was

modelled, which implies a very high cost in resources. Some other studies use models of a 20° sector, being complex models but at the same time having low level of geometrical detail in the studied components, which reduces the accuracy of results [3,4]. In other cases, sector models include the ITER coils but a simplified vacuum vessel [5], or the sub-modeling approach is implemented [6], reducing the resource costs compared to the previous cases but still being complex models. If simplifications, like considering a uniform magnetic (B) field, can be made, and a lower accuracy of results is accepted, a simplified method with a local model can be implemented [7]. Calculation methods to achieve an intermediate accuracy of results without requiring to model a complete reactor sector, minimizing the resource costs, but keeping at the same time a high level of geometrical detail in the components, have not been developed at present, as far as we know.

A complete methodology has been developed to conduct EM analyses by creating algorithms to guide the analyst during the decisions and actions to be taken, from the selection of the case events and the calculation method to the validation of the final results.

This methodology has been applied to the EM analyses of the ex-vessel components of the ITER diagnostic Wide-Angle Viewing System (WAVS) in its final design stage. WAVS is an optical diagnostic to

* Corresponding author.

E-mail address: alejandro.fernandez@ciemat.es (A. Fernández).

provide visible and infrared images and temperature measurements of the internal vessel components for machine protection and scientific analyses [8]. Two independent EM analyses have been carried out for the WAVS ex-vessel components: one for the Optical Hinge and Optical Relay Unit (OH—ORU) components, together with their common support structure, and another one for the Interspace Afocal Module (IAM) [9,10,11,12]. Both, OH—ORU and IAM, are supported by the Interspace Support Structure (ISS) (Fig. 1). The calculation method selected is the Spheres-Worst instant method (Section 4.1), implemented with a 3D finite element model. Intermediate accuracy of results is achieved through the use of a local model with high geometrical definition, as in [7], but also introducing the ISS in the model to consider the influence of flowing induced currents between the component and the structure. The calculated 3D maps of volumetric forces were imported in the corresponding mechanical models to perform the structural analysis and validate their final designs.

The paper includes a verification analysis of the simplifications made, a study of local convergence errors when implementing the T-Omega formulation within the Finite Element Method (FEM) and a method to optimize the resources needed for the EM analysis.

2. Methodology for the selection of the worst case events

Three main types of plasma events are considered for EM analyses, the aforementioned MD and VDE events and the Magnet Fast Discharges (MFD). For ITER, these events are categorized into four levels depending on their expected occurrence (Categories I, II, III and IV) [13]. For the later structural analysis of a component under design, a table of applicable load combinations is created. This table includes all the combinations of inertial, EM, thermal and accidental loads to be considered to validate the component design.

There are dozens of EM events that could be considered to perform an EM analysis, including all subtypes of MD, VDE and MFD events. For example, 18 events were considered for the global EM analysis of the ITER Interspace region of the equatorial port 12 [4]. However, one or two worst case events could be selected to include all the events in the applicable load combinations, especially if the expected EM loads are not design driving.

A method has been developed to select the worst case among the considered EM events. The method quantifies, through simple analytic calculations, the case producing the highest EM forces in the studied component. The methodology is based in the Lorentz Force law and the Faraday-Lenz law. According to these laws the arising force in the studied component will be proportional to the cross product $\mathbf{J} \times \mathbf{B}$, and

the curl of the current density (\mathbf{J}) is proportional to $d\mathbf{B}/dt$. Therefore, the event producing the highest force can be identified by comparing the product $\|d\mathbf{B}/dt\| \cdot \|\mathbf{B}\|$ among the events. To be conservative, this variable is evaluated in the point of the area of the studied component with the highest $\|d\mathbf{B}/dt\| \cdot \|\mathbf{B}\|$. However, a previous check is needed before applying this method. The currents induced depend on the direction of $d\mathbf{B}/dt$ and \mathbf{B} for a specific component geometry. Therefore, $\|d\mathbf{B}/dt\| \cdot \|\mathbf{B}\|$ will identify the highest force only if the direction of the vectors $d\mathbf{B}/dt$ and \mathbf{B} do not change significantly over the transient. In general, the direction change is negligible for components far from the plasma, as it is the case of the ex-vessel components under study.

The methodology, illustrated as an algorithm in the flowchart Fig. 2, can be divided into the following steps. First, having the B field maps of the considered EM events (typically MD and VDE events), check, for every event, the point in the area of the studied component with the highest $\|d\mathbf{B}/dt\| \cdot \|\mathbf{B}\|$. Then, check if the direction change of the vectors $d\mathbf{B}/dt$ and \mathbf{B} is negligible. Evaluate $\|d\mathbf{B}/dt\| \cdot \|\mathbf{B}\|$ in this point throughout the entire transient and select its highest value. The time at which the highest value is reached will be called “worst instant” (t_w). Compare $\|d\mathbf{B}/dt\| \cdot \|\mathbf{B}\|$ at t_w among the events. The one with the highest value will be the worst case event. To check if this event covers all the cases in the applicable load combinations it has to be verified if its type (MD or VDE) includes the other type, for every category, of the load combinations table. If this is verified, then the EM analysis can be performed just for the worst case event. Otherwise, perform the EM analysis for two cases, the worst MD event and the worst VDE event. In this way, when considering the load combinations during the structural analysis phase, the combination cases for every category will be covered either with the worst MD or the worst VDE.

2.1. Application to the EM analyses of the WAVS ex-vessel components

The method described above was applied to the EM analyses of the WAVS ex-vessel components [11]. For these analyses four EM events were considered, two MD and two VDE. The selected point for the evaluation of $\|d\mathbf{B}/dt\| \cdot \|\mathbf{B}\|$ was initially the center of gravity of the IAM and OH—ORU components. To see if this point was appropriate, $\|\mathbf{B}\|$ was evaluated at $t = 0$ ms along the three coordinate axis. As the $\|\mathbf{B}\|$ variation along the radial axis was significant in the area of interest, the point with the highest $\|\mathbf{B}\|$ along the radial axis was conservatively selected. A slightly more conservative point would have been the point with the overall highest $\|d\mathbf{B}/dt\| \cdot \|\mathbf{B}\|$, as proposed in the methodology described in the previous section.

The resulting worst case event, derived from the comparison of $\|d\mathbf{B}/dt\| \cdot \|\mathbf{B}\|$ at t_w among the four cases, was a Major Disruption event called MD_DW_exp16ms_catIII. Following the algorithm of the methodology proposed (Fig. 2), this case was verified to cover all the cases in the applicable load combinations table [11]. Therefore, the EM analyses of IAM and OH—ORU were performed for this MD only, saving important resources comparing to the option of performing the EM analysis for the four considered events.

3. Methodology for the selection of the calculation method and components modelled

The selection of the calculation method highly depends on the study goals and on the characteristics of the imposed B field. As explained before, if these goals and B field conditions require to consider the contributions from global sources, the method frequently includes the model of complete tokamak sectors. On the other hand, assessing the contributions from global sources may not be required, for example, in a preliminary EM analysis (Preliminary Design Review phase) with expected significant EM loads, like in [7], or in a final analysis (Final Design Review phase) with loads not expected to be design driving, as it is our case.

One of the contributions that could be neglected, if justified, is the

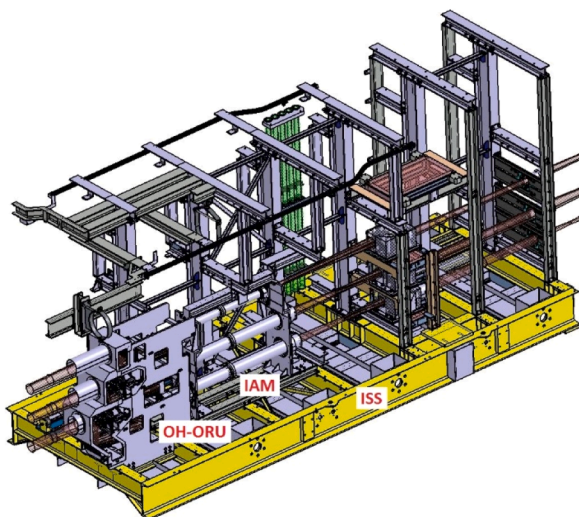


Fig. 1. OH—ORU and IAM attached to the Interspace Support Structure.

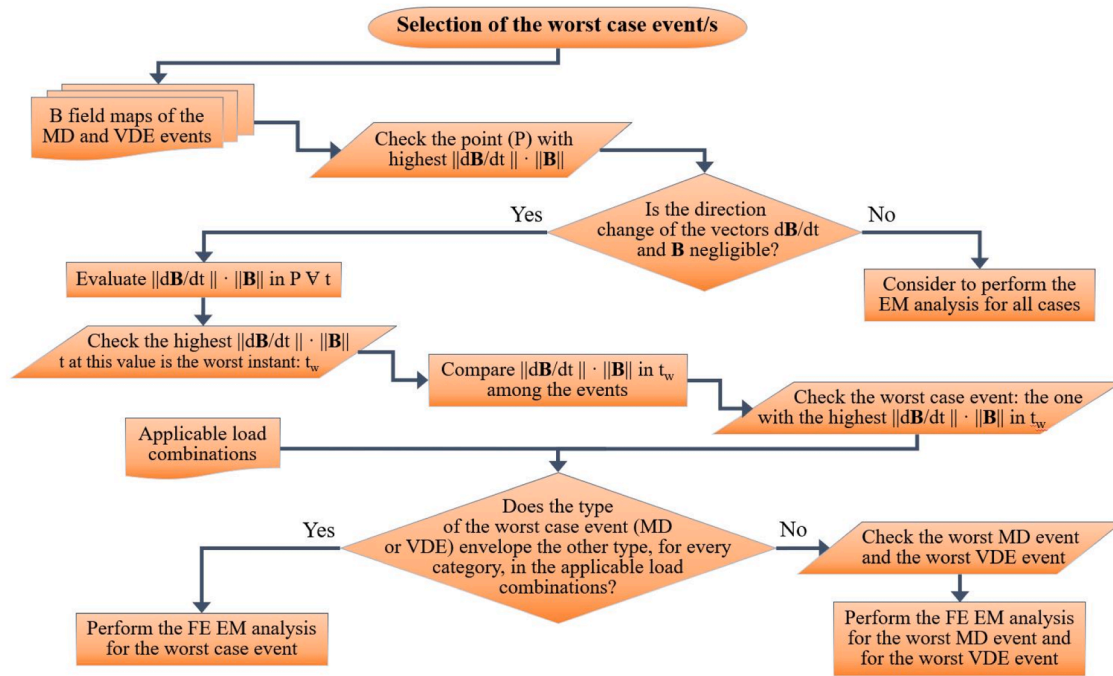


Fig. 2. Flowchart for the selection of the worst case events.

spatial **B** distribution. If a uniform **B** field can be considered, the Spheres-Worst instant method can be selected. The implementation of this method allows the use of local models and a reduced time window, saving a great amount of resources compared to models including complete sectors and simulations of the full transient event. However, if the spatial **B** distribution should be considered, other methods have to be selected, like the sub-modeling approach, for example. The disadvantage of this case is that a spatial **B** distribution is not possible to be modelled in ANSYS-Maxwell without modelling a complete tokamak sector, and introducing all the **B** sources and required model

symmetries, so it is not compatible with local models.

In the case of the selection of the Spheres-Worst instant method, a choice has to be made regarding the components to be modelled. If significant currents flowing between the studied component and the supporting structure or magnetic coupling with other components is not expected, then, the component under study can be modelled alone. Otherwise, an expanded local model should be built, including the structure and components connected to the analyzed component. Nevertheless, in the case of a low accuracy of results required, like in Preliminary Design analyses, the component can be also modelled alone.

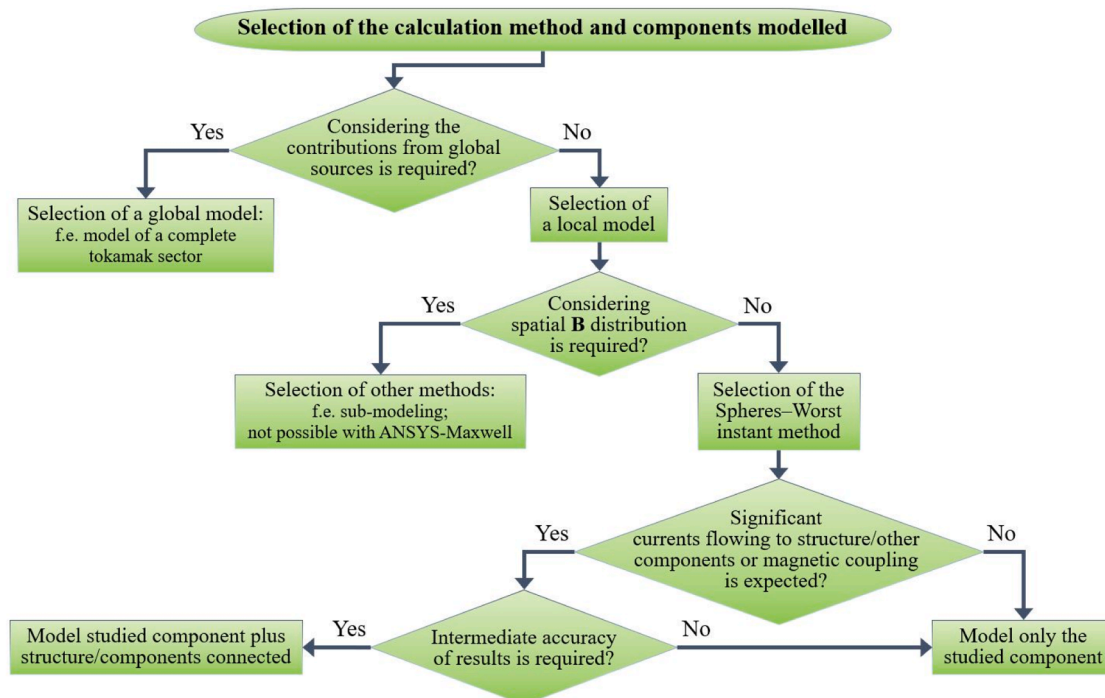


Fig. 3. Flowchart for the selection of the calculation method and components modelled. was verified to be significant [12].

The following flowchart in Fig. 3 shows this methodology as an algorithm.

3.1. Application to the EM analyses of the WAVS ex-vessel components

The selection of the calculation method for EM analyses performed for the WAVS ex-vessel components on its Final Design Review phase followed the described methodology. Due to the characteristics of the environment B field, no design driving EM loads were expected, as usually happens in components located in the ex-vessel area of a tokamak. This condition allowed the use of the Spheres-Worst instant calculation method.

The supporting structure, the ISS, was included in the amplified local models because significant currents flowing to the ISS were expected, due to the bigger dimensions of this structure. Additionally, the analyses aimed to validate final designs, so intermediate accuracy of results were required. To confirm this end, a simulation was performed with a model not containing the ISS, which quantified the relevance of its inclusion in the study. The impact on results of the inclusion of the ISS

4. Methodology for the FE EM analysis with the Spheres–Worst instant method

4.1. The Spheres-Worst instant method

The Spheres-Worst instant calculation method is based on a local model of the selected components, surrounded by three conducting spherical shells which create a uniform, time-varying, B field in their central region, by a defined current flowing through them (Fig. 4). A description of the general method with spheres can be found in [7] and [11].

The implementation of an initial \mathbf{B} and a $d\mathbf{B}/dt$ related to the “worst instant”, already identified during the procedure followed for the selection of the worst case events (Section 2), allows a simulation of a reduced time window, while ensuring conservative results. A selected initial B field evolves in time according to the constant value of $d\mathbf{B}/dt$ at t_w ($d\mathbf{B}_w/dt$). For the selection of the initial \mathbf{B} it has to be checked whether $d\mathbf{B}_w/dt$ would reduce $|\mathbf{B}|$ during the simulation or not. In the case of a negative answer, \mathbf{B} at t_w (\mathbf{B}_w) will be conservatively selected. Otherwise, if using \mathbf{B}_w as an initial condition, the generated \mathbf{B} at the end

of the simulation will be reduced in magnitude, so due to the forces evolving with a weakening B field, obtaining conservative results, compared to a simulation of the full transient event, is not ensured. Instead, an initial \mathbf{B} will be selected to produce the B field from the worst instant at the end of the transient, considering the $d\mathbf{B}_w/dt$ variation (1).

$$B_s = B_w - t_s \cdot d\mathbf{B}_w/dt \quad (1)$$

where \mathbf{B}_s is the selected \mathbf{B} and t_s is the total simulated time.

This procedure for the selection of the \mathbf{B} and $d\mathbf{B}/dt$ simulation parameters can be followed through the right branch of the corresponding flowchart (Fig. 5).

4.2. Creation of a FE 3D model in electronics desktop

To begin with, the CAD model of the selected components is imported in ANSYS to build its Finite Element (FE) model. Simplification and healing of the geometry can be performed with SpaceClaim and DesignModeler ANSYS tools. Then, a volume check is carried out, to ensure that the similarity between the CAD

For the creation of the spherical shells, first, the main dimension of the bounding box of the selected components is checked, in order to get an estimation of the needed size of the spheres. Initially, the diameter of the smallest sphere can be set to three times this main dimension. The spherical shells are drawn with a CAD software and imported in ANSYS to build the FE model.

In parallel, the initial \mathbf{B} and $d\mathbf{B}/dt$ parameters for the simulation are selected, as explained in the previous section, and the equations of the currents to be imposed as inputs in the section of the spheres are created with them [11].

The FE 3D model is created in ANSYS Electronics Desktop putting together the models of the selected components and the spherical shells, the equations of the currents to be imposed in the section of the spheres, and the electrical properties of the materials involved. A FE mesh has to be created for the components, the spheres and the surrounding vacuum region, introducing the corresponding padding, 200 % in our case. The initial size of the mesh elements is estimated according to the required solution accuracy. For example, the ITER accuracy requirement in terms of maximum results deviation in the mesh sensitivity analysis is 5 %.

4.3. Improvement of the baseline FE model

Having an initial EM model in the Electronics Desktop, the ANSYS Maxwell simulation is run. Then, the following checks have to be performed to ensure that the required B field has been simulated with sufficient accuracy. On the one hand, the deviation of $|\mathbf{B}|$ at $t = 0$ ms in the components has to be checked. Obtaining high B field uniformity in the area of interest is easily achieved by controlling the diameter of the spheres. A goal of a maximum $|\mathbf{B}|$ deviation of 0.5 % in this area is proposed. If not reached, the size of the spheres should be increased. On the other hand, the average $|\mathbf{B}|$ at $t = 0$ ms in the components, that is, approximately the $|\mathbf{B}|$ value in the center of the system, is also checked. The simulated $|\mathbf{B}|$ at $t = 0$ ms should be equal to the selected $|\mathbf{B}|$ ($|\mathbf{B}_s|$) defined above. If a significant error in this value is given, correction factors should be derived and introduced in the input equations of the currents [11]. These factors compensate geometrical and discretization errors in the model of the spheres.

After achieving the appropriate B field accuracy, local mesh refinements should be performed, according to the required solution accuracy. This process is carried out in an iterative way, after checking the initial results.

4.4. Sensitivity analyses

Once the improved baseline model is built and baseline results are obtained, sensitivity analyses have to be performed for the mesh and the

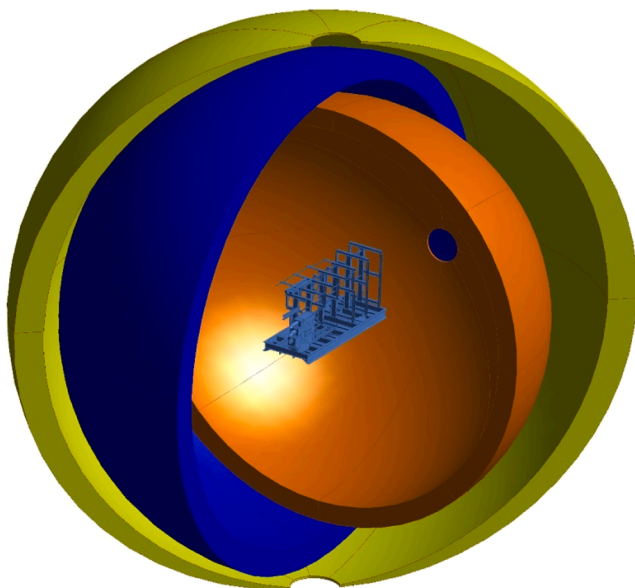


Fig. 4. Example of geometry model for the Spheres-Worst instant calculation: OH—ORU, ISS and the spherical shells.

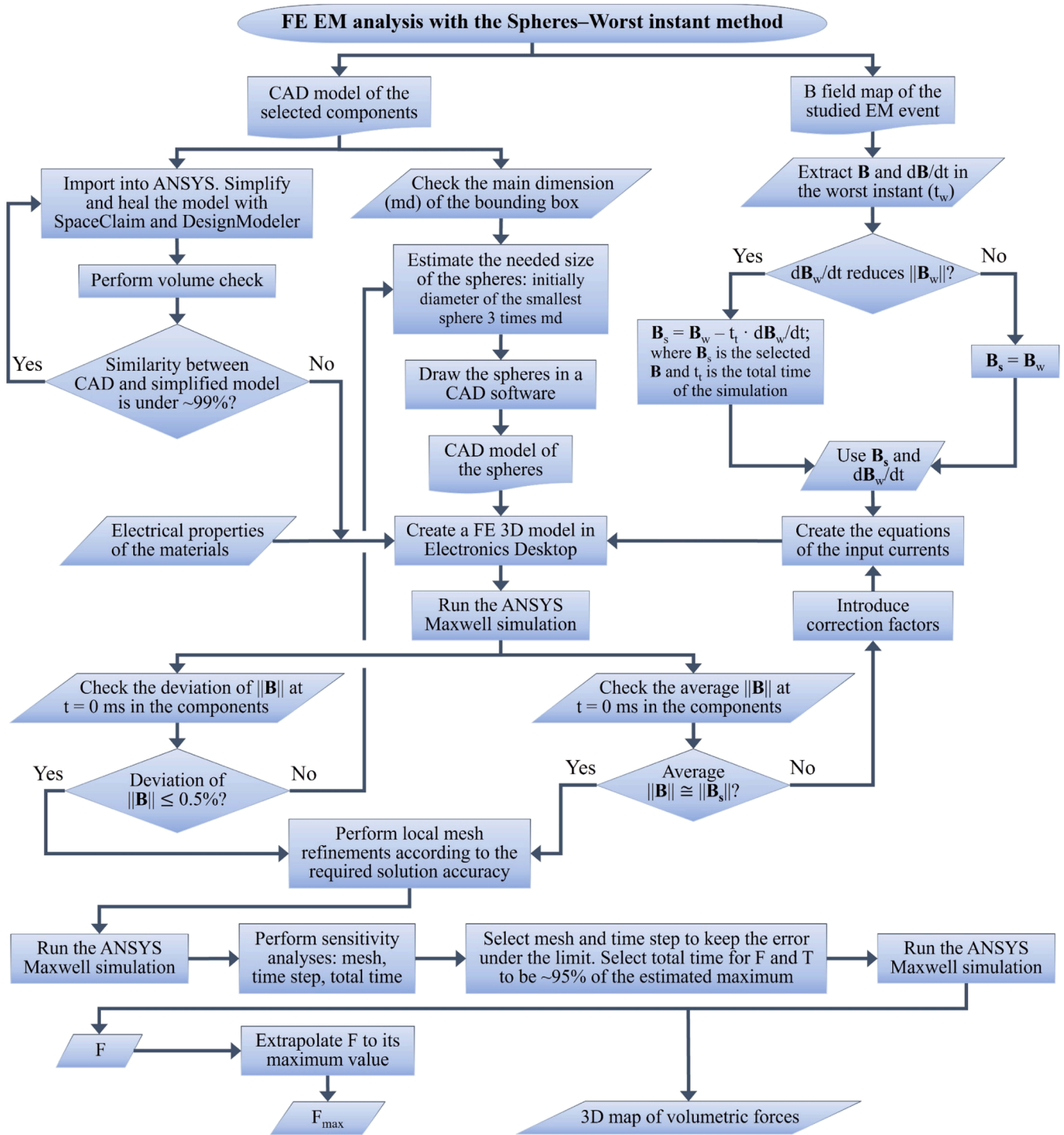


Fig. 5. Flowchart to conduct the FE EM analysis with the Spheres-Worst instant method, and the simplified model is satisfactory. A target of a 99 % similarity was chosen in our case.

time step.

Models with different levels of mesh discretization are compared and results convergence is analyzed. The mesh is selected keeping the relative difference of results under a defined limit. In a similar way, the results convergence is analyzed for the time step size and its selection depends on the required limit. In our case, the ITER requirements imposed a maximum difference in results of 5 %.

4.5. Force curve fit and selection of simulated time

A method has been developed to save simulation resources by minimizing the total simulated time, and extrapolate the results to an estimated maximum, ensuring a conservative solution compared to a simulation of the full transient event.

The system, composed by the metallic components immersed in a varying B field with a constant change rate, behave like an RL circuit with a constant charging voltage (V_C). The following formula (2) describes the current evolution in a charging coil (L).

$$I = I_{max}(1 - e^{-t/\tau}) \quad (2)$$

where $I_{max} = V_c/R$ is the saturated maximum current and $\tau = L/R$ is the time constant of the system, corresponding to the time to charge to a factor $(1 - 1/e)$ of I_{max} .

As the Lorentz force is proportional to the induced current in the components, the resulting simulated F (total force of the studied components) curve can be fitted to the curve of the charging coil shown above (3).

$$F = F_{max}(1 - e^{-t/\tau}) \quad (3)$$

where F_{max} is the estimated maximum force and τ is the time constant of the system.

The fitting can be done by estimating initial values of F_{max} and τ (t for $F = [1 - 1/e] \cdot F_{max}$) and iteratively minimizing the obtained sum of the squared residuals.

Simulated results are iteratively fitted as described above until the current force is, for example, 95 % of the fitted estimated maximum, moment in which the simulation is stopped. This value has been chosen in order to get reliable results while achieving important resource savings. Specifically, the time needed for this force percentage can be around 35 - 40 % less than the time to reach 99 % of the maximum force (see Section 6.2).

4.6. Final results

The conservative result for the total force is the extrapolated F_{max} obtained through the curve fitting explained before.

To introduce the extrapolated results in a mechanical model for the structural analysis the calculated forces have to be divided by 0.95. In ANSYS Mechanical, to import and extrapolate the volumetric forces, a scale factor can be introduced in the settings of the Imported Load tool.

5. Worst instant EM analyses of OH-ORU and IAM

5.1. Description of the initial model

The initial methodology implemented below has been improved, leading to the one described in the previous section.

B_w and dB_w/dt of the MD_DW_exp16ms_catIII event were selected as initial simulation parameters.

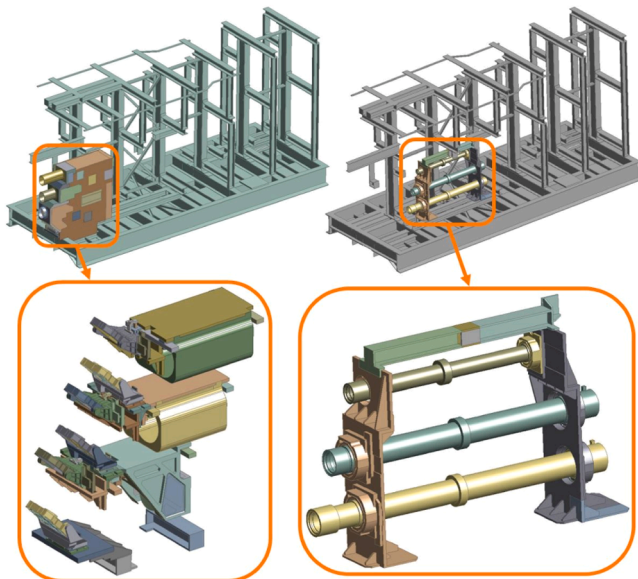


Fig. 6. OH—ORU (left) and IAM (right) models plus details of sub-components.

Two FE models were created in the Electronics Desktop, ANSYS Release 2021 R2, for the OH—ORU and the IAM [11,12], respectively (Fig. 6). The volume check was performed, obtaining a similarity above 99 % in both cases.

For the spherical shells, the diameter of the smallest spheres was selected to be three times of the main dimension of the bounding box of the modelled components, including the ISS. A vacuum region was created with 200 % padding.

The accuracy of the simulated B field was checked after an initial Maxwell simulation. The deviation in the area was under 0.1 % in both cases, so the dimension of the spheres was considered appropriate. On the other hand, correction factors were introduced in the current equations to correct a small error in the average $||B||$ at $t = 0$ ms of around 0.3 %. The overall final error was under 0.1 % in any case.

Sensitivity analyses were performed on the baseline models for the mesh and time step. The relative differences in the final results (global force and torque) were kept under 1.3 % for the OH—ORU and under 2.6 % for the IAM. These values are under the ITER requirement of 5 %.

The total simulated time was selected in 30 ms. A sensitivity analysis was performed comparing the results to a simulation of 40 ms, obtaining an error of 1.3 % in the case of the OH—ORU and 2 % for the IAM.

5.2. Main initial results

The induced currents and volumetric forces results have been published in [11] and [12] and will not be analyzed here. The output forces were imported in the mechanical models, either as net forces by sub-components or as a 3D map of volumetric forces, depending on the specific requirements of the structural analyses.

For the purpose of the present methodological study, the magnitude of the total force of OH—ORU and IAM will be considered (Table 2 and Fig. 9).

6. Improvement and validation of the Spheres-Worst instant method

6.1. Comparison of results of the Full transient vs. Worst instant EM analyses and methodology improvement

A study has been performed to validate the Worst instant simplification made for the OH—ORU and IAM EM analyses, using the B_w and dB_w/dt values from the considered transient event. The study comprises the full transient simulation of the MD_DW_exp16ms_catIII event (Fig. 7) for each model.

The Maxwell models for the Full transient analysis kept the same geometry and mesh from the Worst instant analysis. Regarding the time discretization the transient has been divided in seven time windows

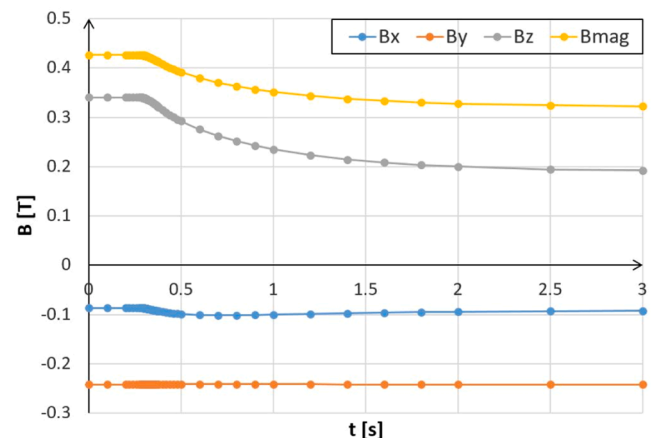


Fig. 7. B field transient for MD_DW_exp16ms_catIII.

(Solution Setups in the Electronics Desktop). A different time step value was defined for each time window, in order to adapt the time discretization to the required solution accuracy in every instant (Table 1). A total of 41 time steps were defined ranging from 0.4 ms to 300 ms.

The computation times of the simulations for the Full transient analyses of OH—ORU and IAM were 41.9 h and 12.3 h, respectively. That means factors 2.3 and 1.8 longer than the Worst instant analyses.

The calculated B field decreases in the models during the transient from an average approximated value of 0.43 T at $t = 0$ ms to a final value around 0.32 T.

The calculated total force reaches its global peak value at $t = 380$ ms for both OH—ORU and IAM (Fig. 8). This result is in agreement with the procedure followed for the selection of the worst instant (Section 2). The highest EM forces appear at $t = 380$ ms as this instant has the highest value of $||d\mathbf{B}/dt|| \cdot ||\mathbf{B}||$, and therefore, it was the worst instant selected to extract the inputs for the Worst instant analyses. A secondary local peak of F appears in both models at $t = 280.4$ ms, when a small toroidal field (B_y) peak caused by the plasma poloidal current is given (Fig. 8). Note that a fine time discretization was set around this local peak in order to capture it (Table 1).

Both, the induced currents and the force density maps at $t = 380$ ms of the transient, are almost identical to the final currents and forces in the Worst instant analyses [11]. The maximum difference between the current density peak values of the Worst instant analyses and the Full transient analyses is 1.1 %. And the maximum difference for the force density peaks is 2.1 %.

The calculated total force at $t = 380$ ms in the OH—ORU is 264.7 N, while in the IAM is 210.3 N. The maximum difference between these results and the results from the Worst instant analyses is 2.1 % (Table 2).

The Worst instant analysis shows a slightly higher (more conservative) force result for the OH—ORU component, as expected. However, the result in the case of the IAM component is lower in the Worst instant analysis than in the full transient simulation (Table 2). Note that the difference between results in any case is small and lower than the ITER requirement of 5 %. An assessment of the simplifications made in the Worst instant analyses was performed to identify the cause of this discrepancy.

In the studied event, $d\mathbf{B}_w/dt$ reduces \mathbf{B} in magnitude (mostly B_z), so at the end of the simplified transient of 30 ms B is 1.6 % lower than at the beginning. As F is proportional to B, setting \mathbf{B}_w as initial condition does not ensure a resulting worst value for F at the end of the simplified transient. A more conservative simplification is the selection of an initial \mathbf{B} to produce \mathbf{B}_w at the end of the simplified transient, considering the $d\mathbf{B}_w/dt$ variation, as described in the methodology presented.

In OH—ORU, the conservative simplification of having the worst value of $d\mathbf{B}/dt$ compensates the non-conservative simplification of having \mathbf{B}_w at $t = 0$ ms. In IAM, the interaction of the currents with the B_z component produces the main force component in the Y direction, because of its geometry and relative position in the ISS. Therefore, the reduction of B_z at the end of the simplified transient impacts highly on the results, more than in the OH—ORU case. F_y in IAM results mainly from the cross product of j_x , which are the highest currents, going along the tubes, times B_z , according to the Lorentz Force formula. Therefore, the non-conservative simplification of the initial \mathbf{B}_w weights more in this case than having the $d\mathbf{B}_w/dt$ conservative value, resulting in a lower F

Table 1
Time discretization settings for the Full transient EM analyses.

Solution Setup	Time window [ms]	Time step [ms]	Number of time steps
1	0 – 280	70	5
2	280 – 282	0.4	5
3	282 – 372	10	9
4	372 – 392	4	5
5	392 – 492	20	5
6	492 – 992	100	5
7	992 – 3092	300	7

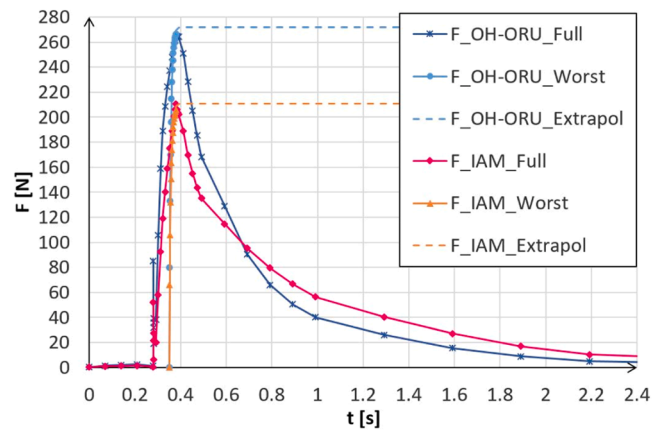


Fig. 8. Total force comparison between the Full transient and Worst instant analyses.

Table 2

Comparison of total force between the Full transient analysis and the Worst instant analysis.

Component	F Full transient [N]	F Worst instant [N]	Difference [%]
OH—ORU	264.7	266.2	0.6
IAM	210.3	205.8	-2.1

result.

In addition, the selected simulated time of 30 ms in the Worst instant analyses implies that the currents are developed to a value about 98 % of their asymptotic value. However, in the Full transient simulation the currents are fully developed when the peak is reached at $t = 380$ ms, because they were under development since at least 100 ms before, when the significant B field variation started. This fact implies an additional small reduction of F in the Worst instant analysis.

In order to confirm this explanation, a simulation of the IAM model was performed, selecting an initial \mathbf{B} to produce the B field from the worst instant at the end of a simplified transient of 40 ms. The result of multiplying the $d\mathbf{B}_w/dt$ variation by 40 ms was subtracted to \mathbf{B}_w . The resulting B field for $t = 0$ ms was $B_x = -0.09$ T, $B_y = -0.242$ T and $B_z = 0.332$ T. The calculated total force at the end of the simplified transient was 213.5 N. This result is 1.5 % higher (more conservative) than the result from the Full transient analysis (Table 2).

Considering this, the already described methodology has been systematized to ensure obtaining conservative results with the Worst instant simplification while minimizing simulation resources. On the one hand, through the selection of an initial \mathbf{B} to produce the highest forces (Section 4.1). On the other hand, with the extrapolation of results through the curve fitting procedure explained in Section 4.5.

6.2. Application of the force curve fit method to the EM analysis of the WAVS ex-vessel components

The resulting simulated F curves for OH—ORU and IAM (Section 5) were fitted through (3) (Fig. 9). F_{max} and τ were initially estimated and final values were derived iteratively (Table 3).

Following the developed method, simulations should be halted when reaching 95 % of F_{max} . This sought force is reached at a simulated time of 22 ms for OH—ORU and 24 ms for IAM, saving 8 and 6 ms of simulated time, respectively, compared to the actual analyses performed with 30 ms. The computation times for the 30 ms analyses were 17 h, 51 min for the OH—ORU (CPU time 23 h, 59 min) and 6 h, 43 min for the IAM (CPU time 9 h, 35 min). As the computation time is roughly proportional to the number of time steps, the time saved would have been around 4 h, 49 min (27 %) for the OH—ORU and 1 h, 21 min (20 %) for the IAM

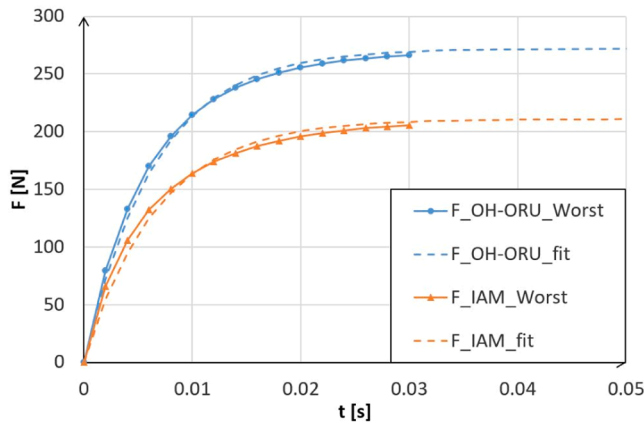


Fig. 9. F curve fit for OH-ORU and IAM.

Table 3

F curve fitting parameters for OH-ORU and IAM.

Component	F_{max} [N]	τ [s]
OH-ORU	272	0.0065
IAM	211	0.0067

Table 4

Estimated savings in computation resources with the optimized method compared to the actual analyses.

Analysis	Simulated time [ms]	% of F_{max}	Computation time [h]	Savings [%]
Actual OH-ORU	30	97.9	17.85	-
Actual IAM	30	97.5	6.72	-
Optimized OH-ORU	22	95.3	13.03	27
Optimized IAM	24	95.4	5.37	20

(Table 4). The analyses were performed in a workstation with 512 GB of RAM memory and dual Intel Xeon Gold processors (12 cores, 3.00 GHz each). The settings in ANSYS HPC Options limited the number of cores to 8 and RAM to 90 %, to allow parallelization. Comparing the resources needed for the 95 % of F_{max} to the resources to reach 99 %, the savings are around 39 % for OH-ORU and 37 % for IAM.

6.3. Study of local convergence errors due to the implementation of the T-Omega formulation with FEM

The T-Omega formulation for FEM is widely used for electromagnetic calculations, being the default formulation for the ANSYS Maxwell solver.

The identification of convergence errors in inner boundary edges and corners, due to the unfeasibility of satisfying at the same time the boundary conditions and the T-Omega formulation, was published in previous works [11,14].

Further investigation has been carried out regarding this matter, through simulations of a local subcomponent model, the OH mirror called OH-2, with different mesh settings (Fig. 10).

Being an isolated local model, the net electromagnetic force should be zero. However, due to the formulation errors explained above, the divergence of the B field is different from zero in edges and corners, resulting in arising currents and forces. For a base model with 27,979 mesh elements in the subcomponent, the total force was 0.246 N instead of zero. This problem can be mitigated by creating a mesh which ensures to have at least two layers of mesh elements in every piece. In this way, these layers add degrees of freedom which help the field to satisfy the

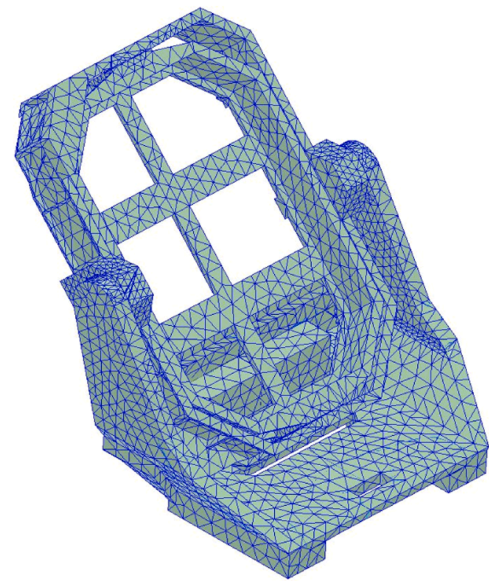


Fig. 10. Base model of the OH-2 tangential right LoS.

boundary conditions and be properly represented. For a model with 65,209 mesh elements, having ensured that every piece have at least two layers of elements, the resulting force is 0.006 N, considered negligible. To check that this result is due to the given explanation and not just because of the increased number of mesh elements, another model was created with higher number of elements, but without ensuring that every piece has two layers of elements. In this case, with 113,058 mesh elements, the force was almost the same as the base model, 0.241 N.

7. Conclusion

A complete methodology has been developed to conduct EM analyses by creating algorithms to guide the analyst during the decisions and actions to be taken, from the selection of the case events and the calculation method to the validation of the final results.

The methodology can be divided into three main steps. The first step is the selection of the worst case among the considered EM events. The second one, the selection of the calculation method and components modelled. The last step is the FE EM analysis with the selected method, the Spheres-Worst instant method in our case. This calculation method has been thoughtfully developed and its procedure explained step by step.

This methodology has been applied to the EM analyses of the ex-vessel components of the WAVS diagnostic in its final design stage.

A study has been performed to validate the Worst instant simplification made for the OH-ORU and IAM EM analyses by performing the Full transient simulation of the MD_DW_exp16ms_catIII event for each model. The lessons learned from the analysis of results led to the improvement and optimization of the calculation method. Moreover, the issue of local convergence errors due to the implementation of the T-Omega formulation with FEM, identified in previous works, has been further investigated. A mitigation action, based on ensuring the creation of the mesh with at least two layers of elements, has been proposed and demonstrated.

The resources savings with this methodology are significant. The application of the force curve fit method to the performed EM analyses of the WAVS components would have implied savings between 20 % and 27 % of the computation time. Moreover, the actual time savings in the Worst instant EM analyses were around 45 %, compared to the analyses of the Full transient event. These savings are of great importance when dealing with heavy FEM EM models which run in time orders between hours and days.

Disclaimer

The work leading to this publication has been partially funded by Fusion for Energy Grant Agreement F4E-GRT-1146. This publication reflects the views only of the author, and Fusion for Energy cannot be held responsible for any use which may be made of the information contained therein.

CRedit authorship contribution statement

A. Fernández: Writing – review & editing, Writing – original draft, Methodology, Investigation, Formal analysis, Data curation, Conceptualization. **J. Martínez-Fernández:** Writing – review & editing, Validation, Supervision, Methodology, Investigation, Conceptualization. **M. Medrano:** Writing – review & editing, Supervision, Resources, Project administration, Funding acquisition. **S. Cabrera:** Writing – review & editing, Validation, Resources. **P. Testoni:** Writing – review & editing, Validation, Supervision, Project administration, Conceptualization. **E. Rodríguez:** Writing – review & editing, Validation, Supervision, Resources.

Declaration of competing interest

The authors declare the following financial interests/personal relationships which may be considered as potential competing interests:

Alejandro Fernandez Navarro reports financial support was provided by Fusion for Energy. If there are other authors, they declare that they have no known competing financial interests or personal relationships that could have appeared to influence the work reported in this paper.

Data availability

The authors do not have permission to share data.

References

- [1] P. Testoni, et al., F4E studies for the electromagnetic analysis of ITER components, *Fusion Engineering and Design* 89 (2014) 1854–1858, <https://doi.org/10.1016/j.fusengdes.2014.01.082>.
- [2] C. Feng, et al., Numerical simulation on the eddy current electromagnetic forces and the mechanical reliability of ITER in wall shielding blocks induced by plasma disruption events, *Fusion Engineering and Design* 174 (2022) 112972, <https://doi.org/10.1016/j.fusengdes.2021.112972>.
- [3] J. Guirao, et al., Electromagnetic analysis of ITER generic equatorial port plug designs during three plasma current disruption cases, *Fusion Engineering and Design* 87 (2012) 141–155, <https://doi.org/10.1016/j.fusengdes.2011.11.013>.
- [4] S. Iglesias et al., EM Analysis of ISS (Eq12), ITER IDM internal Report (4FYRSR v1.0), 2020.
- [5] D. Giorla, et al., EM zooming procedure in ANSYS Maxwell 3D, *Fusion Engineering and Design* 132 (2018) 67–72, <https://doi.org/10.1016/j.fusengdes.2018.04.096>.
- [6] P. Testoni, et al., A sub-modeling approach for the electromechanical disruption analysis of the ITER ICH antenna, *Fusion Engineering and Design* 83 (2008) 695–701, <https://doi.org/10.1016/j.fusengdes.2008.03.003>.
- [7] S. Garitta, et al., Electromagnetic analysis of ITER equatorial Wide Angle Viewing System (WAVS) in-vessel components, *Fusion Engineering and Design* 170 (2021) 112471, <https://doi.org/10.1016/j.fusengdes.2021.112471>.
- [8] Reichle, et al., Concept development for the ITER equatorial port visible/infrared wide angle viewing system, *Review of Scientific Instruments* 83 (2012) 10E520, <https://doi.org/10.1063/1.4734487>.
- [9] C. Pastor, et al., Optical design of ex vessel components for the Wide Angle Viewing System diagnostic for ITER, *Fusion Engineering and Design* 168 (2021) 112607, <https://doi.org/10.1016/j.fusengdes.2021.112607>.
- [10] M. Medrano, et al., Design overview of ex vessel components for the Wide Angle Viewing System diagnostic for ITER Equatorial Port 12, *Fusion Engineering and Design* 168 (2021) 112651, <https://doi.org/10.1016/j.fusengdes.2021.112651>.
- [11] A. Fernandez, et al., Electromagnetic Analysis of the Interspace Afocal Module of the Wide Angle Viewing System diagnostic for ITER, *Fusion Eng. Des.* 191 (2023) 113592, <https://doi.org/10.1016/j.fusengdes.2023.113592>.
- [12] A. Fernandez, et al., Electromagnetic analysis of the ITER wide angle viewing system components with a simplified approach, *Fusion Eng. Des.* 205 (2024) 114562, <https://doi.org/10.1016/j.fusengdes.2024.114562>.
- [13] G. Sannazzaro et al., Load Specifications (LS), ITER IDM internal Report (222QGL v6.2), 2017.
- [14] K. Preis, et al., Gauged Current Vector Potential and Reentrant Corners in the FEM Analysis of 3D Eddy Currents, *IEEE Transactions on Magnetics* 36 (4) (2000). VolNo, <https://ieeexplore.ieee.org/document/877575>.